IL NUOVO CIMENTO VOL. 18 D, N. 6 Giugno 1996

Experimental study of X-ray generation in laser-produced plasmas based on *K*-shell time-resolved spectroscopy

A. MACCHI [1], D. GIULIETTI [2], S. BASTIANI [1] (*)
A. GIULIETTI [1] and L. A. GIZZI [1]

[1] *Istituto di Fisica Atomica e Molecolare - Via del Giardino 7, 56127 Pisa, Italy*
[2] *Dipartimento di Fisica, Università di Pisa - Piazza Torricelli 2, Pisa, Italy*

(ricevuto il 12 Dicembre 1995; approvato l'8 Gennaio 1996)

Summary. — Soft–X-ray generation in aluminium plasmas produced by Nd nanosecond laser pulses is investigated analysing time-resolved spectra of *K*-shell line emission. Time histories of line emission and electron temperature as well as the time-integrated X-ray yield were studied as a function of laser pulse duration and target position along the laser beam propagation axis. The experimental results suggest that X-ray emission is influenced by self-focusing of laser light in the plasma.

PACS 52.25 – Plasma properties.
PACS 52.50 – Plasma production and heating.

1. – Introduction

At temperatures of hundreds of eV typical of laser-produced plasmas (LPP), the energy emitted in the X-ray region of the spectrum is a relevant percentage of the laser energy. X-ray spectroscopy and imaging are extensively used as a diagnostic of laser-produced plasmas [1, 2]. X-rays can access high-density regions in LPPs, thus allowing the study of the dense plasma region, in which energy transport takes place, as well as the «coronal» region in which the plasma couples with laser light. The spectral features of both line and continuum emission can give information on plasma conditions; *K*-shell spectra have been extensively studied and modelled, due to the relative simplicity of the atomic configuration. Since LPP parameters vary in time, time-resolved spectroscopy is essential for detailed studies of LPP. X-ray spectra with high temporal resolution can be obtained using a crystal spectrograph coupled with an X-ray streak-camera [3] or an X-ray framing camera [4]. The temporal evolution of the plasma parameters (temperature, density, radiative opacity) can be

(*) Presently at Laboratoire pour l'Utilisations des Lasers Intenses, Ecole Polytechnique, 91128 Palaiseau Cedex, France.

determined from the analysis of such time-resolved spectra, allowing to characterise coronal plasmas for interaction studies [5], to measure mass ablation rates [6, 7] and to study radiative energy transport [8] in laser-irradiated targets.

On the other hand, LPPs are now extensively used as bright X-ray sources for many different application purposes, including X-ray microscopy, microlithography, EXAFS, microradiography, radiobiology. In order to optimise these X-ray sources for such a variety of applications, a number of broad phenomenological studies have been in progress for more than ten years [9-14]. It has been proven, for example, that the X-ray conversion efficiency of laser light strongly depends upon the atomic number of the target material, the parameters of the laser pulse and the focusing conditions, including the target position with respect to the focused beam waist.

The present work investigates some of the above-mentioned properties of LPP X-ray sources by means of time-resolved spectroscopy. The use of this plasma diagnostic gives an insight into the physical mechanisms of X-ray conversion of the input laser energy with the underlying aim to develop phenomenological «recipes» for the optimisation of X-ray sources.

In this paper we present time-resolved spectra of *K*-shell line emission from plasmas produced by Nd laser light focused on an aluminum target. The spectra show that the X-ray line emission is temporally modulated on a time scale of tenths of picoseconds as the input laser pulse, and that its overall duration is shorter than the laser pulse duration. The temperature of the X-ray–emitting plasma region is evaluated by comparing line intensity ratios with the calculations of a collisional-radiative equilibrium (CRE), steady-state atomic-physics code [15]. The effect of line emission opacity and steady-state approximation on the temperature evaluation is discussed in detail.

The plasma temperature and the time-integrated X-ray yield are studied as a function of target position with respect to the focused laser beam waist and for laser pulses of different duration. Both the X-ray yield and the temperature of the emitting plasma have a maximum in a target position displaced from the nominal focused beam waist, in the direction of propagation of the laser beam; it is shown that, in our experimental conditions, this is not a pure geometrical issue. This effect and the particular dependence of the X-ray yield upon laser pulse energy and duration suggest that X-ray conversion efficiency is influenced by self-focusing of laser light in the plasma. This conclusion is supported by analogies with previous studies of self-focusing, based on optical time-resolved spectroscopy and imaging.

2. – Experimental set-up

The experimental set-up is shown in fig. 1. The plasma was produced by Nd laser pulses ($\lambda = 1.064\ \mu m$) focused on an Al cylinder. The pulse duration was either 3 ns or 20 ns (FWHM). The pulse energy was typically 1.5 J for 3 ns pulses and 5 J for 20 ns pulses. Laser energy and pulse shape were monitored shot by shot using a fast photodiode and a calorimeter.

The laser was transversally monomode but longitudinally multimode. Due to mode beating in the oscillator cavity, the laser emission had a spiky structure with large intensity modulations in the pulse envelope; the duration of the spikes was of the order of $1/\Delta\nu \approx 50$ ps, where $\Delta\nu = 2 \cdot 10^{10}$ Hz is the measured bandwidth.

The laser beam was focused on the target by a $f/8$ lens and at an incidence angle of

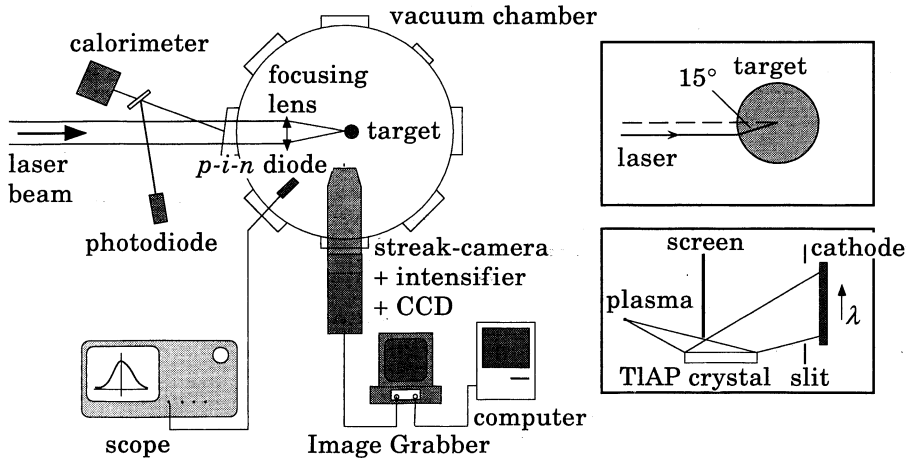

Fig. 1. – Experimental set-up. The angle of incidence of the laser beam on the target and the setting of the TlAP crystal with respect to the streak-camera cathode are shown in separate frames.

15 degrees, to avoid back reflections from the plasma critical surface. The FWHM of the laser spot was approximately 60 μm, which in the case of 3 ns pulses resulted in a nominal intensity on target of the order of $2 \cdot 10^{13}$ W cm^{-2}.

Time-resolved spectra were obtained using a flat TlAP crystal, set in a first-order Bragg configuration, coupled with a streak-camera fitted with a CsI photocathode. The streak-camera was coupled with an image intensifier, a CCD camera and a digital read-out system (Image Grabber), allowing for an on-line acquisition and analysis of experimental spectra. The temporal resolution was 30 ps, 100 ps or 500 ps, depending on the choice of the streak speed and of the width of the slit in front of the cathode. Spectral resolution was determined by both the size of the emitting plasma region and the spatial resolution of the streak-camera imaging system.

The X-ray intensity was measured using an X-ray *p-i-n* diode with a response time of 5 ns and a spectral sensitivity ranging from 0.5 to 10 keV. The investigated spectral window was determined by the product of the diode sensitivity and the spectral transmittivity of the beryllium filters placed in front of the diode.

3. – Experimental results

3·1. *Spectra from plasmas produced by* 3 ns *pulses.* – It was previously found [10, 16] that X-ray emission intensity strongly depends upon the target position on the laser beam propagation axis (hereafter labelled as the x-axis) with respect to the focused beam waist. Thus, we measured the X-ray yield collected in the p-i-n diode for different positions of the Al target on the x-axis, and for an almost constant value of the laser energy. We will identify the $x = 0$ position with the focused beam waist and we will consider x increasing in the direction of propagation of the laser beam. The waist position was determined using two independent methods with an uncertainty of ± 200 μm, well below the measured longitudinal depth of focus (≈ 600 μm).

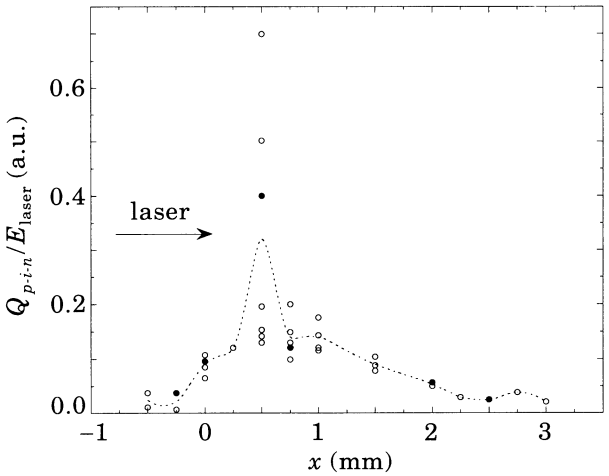

Fig. 2. – Ratio between the charge collected in the *p-i-n* diode and the laser energy (in arbitrary units) *vs.* target position, for 3 ns pulses. The data marked by full dots were taken at the same shots of the spectra shown in fig. 3. ··· Mean.

Figure 2 shows the ratio between the total charge collected in the *p-i-n* diode and the laser energy (which gives a relative measure of the X-ray conversion efficiency) *vs.* x. The laser energy was 1.2 J ($\pm$ 10%). The six dark circles correspond to the six spectra shown below. The filter in front of the *p-i-n* diode was a 30 μm Be foil. Taking into account the transmittivity of the beryllium filter, the spectral sensitivity of the *p-i-n* diode and a simulated emission spectrum of the Al plasma [17], most of the detected X-ray radiation is expected to lie in the spectral region above $\approx$ 1 keV and to consist mainly of *K*-shell line and recombination radiation. Actually, it is known that in the position corresponding to maximum X-ray yield a «hard» X-ray component with an energy of several keV is generated by the bremsstrahlung of suprathermal electrons produced by damping of plasma waves [18]; however, the intensity of the hard component is much less than the intensity of the soft component and thus its contribution to the *p-i-n* diode signal is negligible.

The maximum X-ray conversion efficiency of laser energy was found in the position $x = +0.50$ mm. In this position the experimental data points are largely scattered with respect to the mean value. We also notice that the X-ray yield is sensitive to a target displacement shorter than the focal depth. Furthermore, by varying the laser energy, the dependence of X-ray yield upon laser energy in the $x = +0.50$ position was found to be more than quadratic, as already observed in [18].

In order to further investigate the effect of target position on the X-ray yield, some time-resolved spectra were obtained at different positions of the target on the x-axis. Figure 3 shows a series of spectra obtained in a set of positions containing the centre of the laser waist ($x = 0.00$) and the maximum of X-ray yield ($x = +0.50$). The values of the X-ray yield corresponding to these spectra are evidenced by full dots in fig. 2.

The spectra show resonance lines from Al XII ions up to the He-γ line and the Ly-α resonance line from Al XIII ions. The He-α line is merged with the

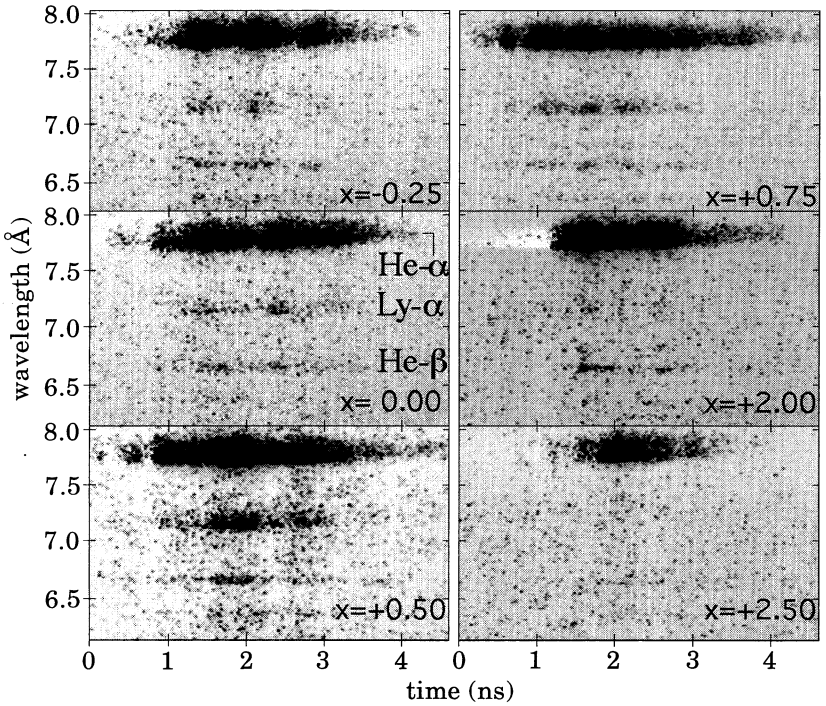

Fig. 3. – Time-resolved X-ray spectra from plasmas produced by 3 ns laser pulses, for different target positions. The identification of the main emission lines is shown.

neighbouring intercombination line and it is saturated, its intensity being much higher than the other emission lines. The temporal resolution is 120 ps. The origin of the time axis is arbitrary and has no physical significance.

Some general features of the spectra can be noticed in fig. 3. In the positions close to the waist, where the highest laser intensity is expected, the X-ray emission has a longer duration and a stronger intensity. The histories of line emission show temporal modulations due to the spiky structure of the laser pulse; the apparent duration of the X-ray emission spikes is determined by the temporal resolution. The actual duration of the spikes was estimated by spectra with higher temporal resolution and was 50–100 ps, of the same order of the laser spikes duration. Thus, line emission appears to follow closely the temporal modulations in the laser pulse. Far from the beam waist ($x = +2.00$ and $x = +2.50$), both the X-ray intensity and the emission duration decrease. This can be explained by the large focal spots, and thus the low irradiation intensity, at these displacements from the waist. In these conditions appreciable X-ray emission is only observed in correspondence of the most intense laser spikes, thus the emission has a shorter duration and a more evident spiky structure. The whole duration of X-ray line emission, defined as the FWHM of the envelope of the temporal profile, is less than 2 ns for every spectral line and in every target position and thus it is definitely shorter than the laser pulse duration.

The dependence of the plasma electron temperature (T_e) upon the target position can be deduced from the ratio between the Ly-α and the He-β line intensities, which increases with T_e. It can be noticed in fig. 3 that the Ly-α intensity relatively to the

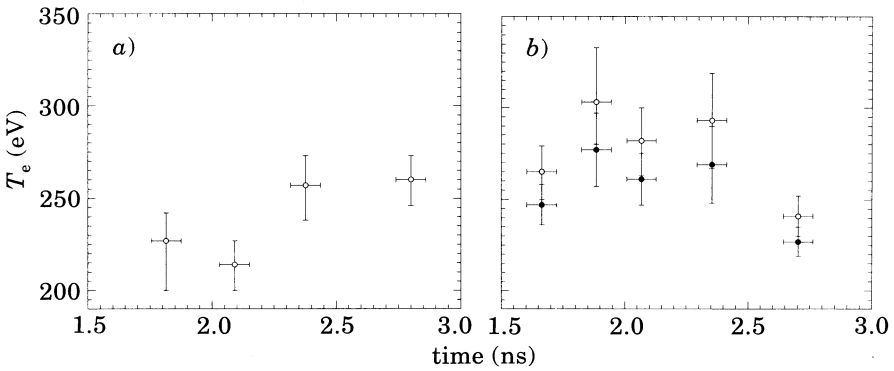

Fig. 4. – Time history of electron temperature *a*) in the $x = 0.00$ position, for a plasma size of 60 μm and *b*) in the $x = +0.50$ position, for a plasma size of both ○ 60 μm and ● 100 μm.

He-β intensity appears to have a maximum in the $x = +0.50$ position. This suggests that the temperature of the X-ray source is higher at the position of maximum X-ray yield than at the beam waist, where a higher laser intensity is expected. Far from the waist, the He-β line becomes more intense than the Ly-α line; thus the plasma is found to be definitely colder in these target positions.

The electron temperature of the plasma region from which *K*-shell emission originates can be evaluated by comparing the Ly-α to He-β line ratio with the calculations of the atomic physics code RATION [15]. This code solves the ionic rate equations assuming CRE and calculates the dependence of line ratios upon T_e and n_e for a homogeneous plasma of a given size, including opacity effects. In order to evaluate T_e, the experimental Ly-α to He-β line ratio, evaluated from the spectra at various instants, was compared with the simulated line ratio, calculated as a function of T_e and for $n_e = 10^{21}$ cm^{-3}. This value is consistent with measurements of density-sensitive intercombination-to-He-α resonance line ratio and Ly-α satellite lines ratios in time-integrated spectra with improved spectral resolution [19]. The effect of different electron densities (between an order of magnitude) on the evaluation of T_e was found to be less important than either the uncertainty due to the experimental error on the line ratio or to different choices of the opacity level (as discussed below).

Figures 4*a*) and *b*) show the temporal evolution of the electron temperature corresponding to the Ly-α-to-He-β line ratio for two spectra in fig. 3, taken in the $x = 0.00$ mm and $x = +0.50$ mm position, respectively. In order to obtain the line ratio, the spectrum lineout was integrated over an interval of 120 ps, corresponding to the temporal resolution.

The electron temperature obtained in this way depends upon the value of the plasma size assumed in the RATION simulations; in fact, the plasma opacity is determined by the plasma size as well as other plasma parameters. The size of the emission region could be estimated from time-integrated X-ray pin-hole images of the source [19], in a spectral window similar to that of the spectrometer. In the waist position a size of 60 μm, which also corresponds to the measured laser beam waist diameter, was then assumed. In the $x = +0.50$ mm position we also show the values of T_e obtained for a plasma size of 100 μm, in order to discuss the effect of different opacity levels on the temperature determination. From fig. 4*b*) it is clear that the

larger value of the plasma size would lead to a lower temperature for the same line ratio.

The CRE model assumes that the rate equations for the atomic levels can be solved in the steady-state approximation. Let us now discuss the limits of this assumption in the evaluation of T_e. The conditions required for the steady-state model to hold are fulfilled if the timescale for the hydrodynamic variables T_e, n_e is longer than the characteristic relaxation time for atomic processes in the plasma. In order to evaluate the atomic relaxation time, we notice that in the present temperature regime most of the plasma ions are in the ground states of Al XII and Al XIII ions and that processes coupling levels of the same ionization state are faster than ionization and recombination processes between adjacent ionization states. Thus we need only to evaluate the relaxation time for ionization equilibrium between Al XII and Al XIII ions, neglecting ionization and recombination of other ionization states. This relaxation time τ can be evaluated as

$$\tau = [n_e(S + \alpha_r + \alpha_d + n_e\alpha_{3b})]^{-1} ,$$

where S is the ionization rate for the Al XII ion and α_r, α_d, α_{3b} are, respectively, the radiative, dielectronic and three-body recombination rates for the Al XIII ion. Expressions for these rates were found in the literature (see references in [15] for example). For $n_e \geq 10^{21}\,\mathrm{cm}^{-3}$, $100\,\mathrm{eV} < T_e < 1000\,\mathrm{eV}$, we find $\tau < 10\,\mathrm{ps}$. This realxation time is not only shorter than the overall duration of the laser pulse, but also shorter than the duration of the laser spikes. Thus we expect that the steady-state conditions are satisfied. This is consistent with the observation that line emission appears to follow quickly the temporal modulations of the laser pulse. Incidentally it is interesting to notice that, among the different ionization and recombination processes, dielectronic recombination is very effective [20] and strongly influences the relaxation time.

It is important to notice that τ depends substantially upon the electron density; we expect CRE to be satisfied in the overdense plasma region ($n_e \geq 10^{21}\,\mathrm{cm}^{-3}$) but not necessarily in the expanding low-density corona. If K-shell radiation is emitted mostly from the overdense region, the CRE assumption in the analysis of the spectra is justified. However, if the steady-state assumption were not strictly valid in our case, the electronic temperature deduced from the line ratio could be different from the plasma hydrodynamic temperature. In this case, since we are more interested in the relationship between X-ray emission and laser energy deposition mechanisms than in accurate plasma characterization, we may regard the «CRE temperature» as an effective temperature, whose temporal variations account for plasma heating and cooling during the hydrodynamic evolution. In particular, our observations about the relative dependence of plasma temperature upon the target position remain valid.

3·2. *Spectra from plasmas produced by* 20 ns *laser pulses.* – The measurements described in the previous section were carried out also on plasmas produced by 20 ns laser pulses. In this case the temporal resolution of the spectra was 500 ps. The laser pulse energy was about 5 J, thus the nominal irradiation intensity, with a 60 μm laser spot, was about $1 \cdot 10^{13}\,\mathrm{W\,cm}^{-2}$.

The dependence of the X-ray yield upon the target position is shown in fig. 5. The laser energy was 5.3 J (± 8%). The results are very similar to those

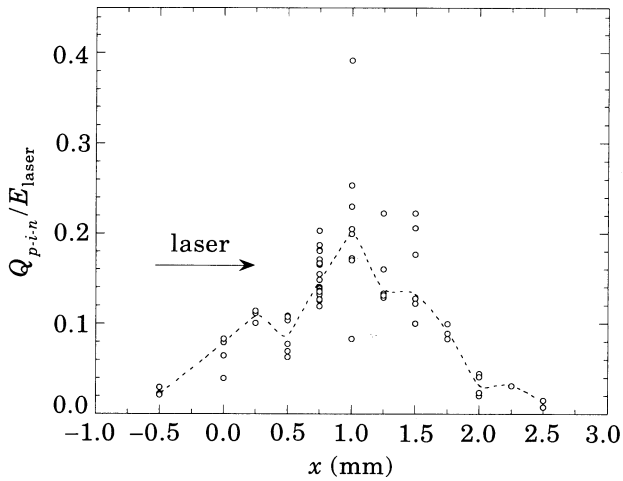

Fig. 5. – Ratio between the charge collected in the *p-i-n* diode and the laser energy *vs.* target position, for 20 ns pulses.

outlined in subsect. 3·1 for 3 ns laser pulses, but with the maximum conversion efficiency position located in the $x = +1.00$ mm position.

A typical time-resolved spectrum, taken at $x = +1.00$ mm and in the same energy range, is shown in fig. 6. This spectrum reveals several interesting features and differences from the spectra obtained with 3 ns pulses. The duration of line emission is shorter than the laser pulse duration also in this temporal regime. The Ly-α line is weaker than the He-β line, showing that the electron temperature is now lower, as is expected from the lower laser intensity.

The Al XI (Li-like) satellite lines on the longer-wavelength side of the He-β resonance line (which are merged in a single spectral structure) appear very intense; the satellite lines of the Ly-α line are also visible. This can be related to the relatively low electron temperature, which causes both a lower plasma ionization degree and makes dielectronic recombination more effective in populating the doubly excited

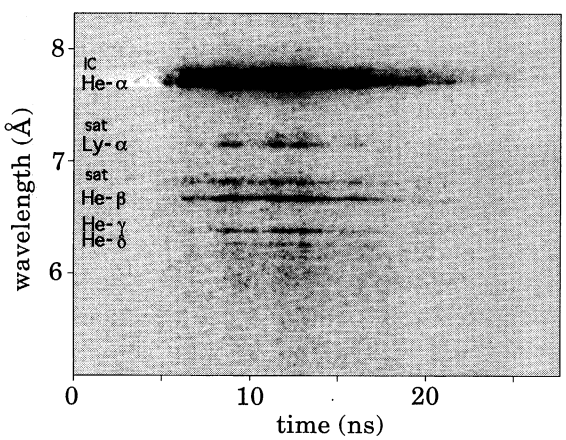

Fig. 6. – Time-resolved spectrum from plasma produced by a 20 ns laser pulse.

states that give rise to satellite line emission. In fact we note that when the plasma temperature decreases the dielectronic recombination rate increases and the process becomes eventually more important than radiative recombination [20].

The electron temperature was estimated as described in the previous section and resulted typically between 150 eV and 200 eV. Those values are consistent with the qualitative considerations outlined above. The maximum temperature was observed with the target in the maximum X-ray conversion efficiency position. This result is analogous to that found in the case of 3 ns pulses.

4. – Discussion

The analysis of *K*-shell line intensity ratios from time-resolved spectra, taken at different positions of the target with respect to the nominal focused beam waist, showed that where the X-ray yield has a maximum the plasma temperature has a maximum too.

In order to understand this effect, it is first shown that the increase in the X-ray yield as the target is displaced from the focused beam waist is not a pure geometrical issue. According to a «geometrical» explanation, when the target is displaced from the waist, a larger volume of the X-ray source would be expected, provided that the laser intensity was held over some «threshold» value necessary to have X-ray emission. If the laser intensity falls below this «threshold» value, as it would certainly happen at large displacements from the waist, the X-ray yield would dramatically decrease. Thus the X-ray yield would have a maximum with the target displaced from the focused beam waist.

An analysis of the actual dependence of the X-ray source size upon the position of the target shows that this explanation does not apply to the present experimental conditions, almost for the case of 3 ns laser pulses. In fact, pin-hole images of the X-ray source for different positions of the target showed that the source size does not vary significantly displacing the target from the focused beam waist to the $x = + 0.50$ mm position. This is consistent with equivalent plane images of the laser spot along the beam axis [21], which showed that between those positions the spot actually changes its shape, due to laser beam astigmatism, but the spot area is about the same, thus for both positions a similar value of the laser intensity is expected.

The fact that the source size remains the same in the $x = + 0.50$ mm position also implies that the increase of the Ly-α–to–He-β line ratio is actually due to an increase of the plasma temperature in this position and it is not due to a different opacity level with respect to the $x = 0.00$ position. In fact the observed Ly-α–to–He-β line ratio in the spectrum taken at $x = + 0.50$ could correspond to a temperature comparable to the temperature measured in the $x = 0.00$ position only if the source size was assumed to be much larger than 100 μm (see fig. 4*b*)). As we discussed above, such an increase of the source size is not observed.

Hence in our experimental conditions the plasma temperature seems to play an important role in determining the soft–X-ray conversion efficiency in the laser-produced plasma. In the position of maximum X-ray yield a hotter plasma is produced, suggesting that a larger fraction of the input laser energy must be absorbed. In order to give an explanation for this, we notice that the observed features of the X-ray conversion efficiency show some significant analogies with a

previous study [21] on laser light filamentation in the long-scalelength expanding plasma, diagnosed by second-harmonic (SH) emission. In that study a similar dependence of SH yield upon target position and laser energy was observed and correspondingly a transition to a filamentary regime was evidenced. The filamentation actually occurred near the $x = +0.50$ mm position and both the growth of filaments and the second-harmonic yield were sensitive to target displacements below the measured depth of focus. Correspondingly a whole-beam self-focusing (SF) effect was also observed; this effect reduced the focal spot size by roughly a factor of two. Both local and whole-beam effects were satisfactorily explained by thermal SF theory [22]. The analogy between that study and the results of the present paper suggest that the X-ray emission may also be strongly influenced by the SF process.

In the case of 20 ns laser pulses, the maximum X-ray yield is in the $x = +1.00$ mm position (fig. 5). In this position the laser spot size is roughly two times larger than in the waist. Thus in this position the increased plasma volume could contribute to the increase in the X-ray yield. However, the plasma temperature is lower at $x = 0.00$ than at $x = +1.00$. This fact is remarkable because in the latter position the nominal laser intensity is expected to be lower than in the waist. Thus we believe that SF strongly contributes to X-ray yield also in the case of 20 ns pulses. This is consistent with the observed displacement of the maximum X-ray yield position from the waist, which is larger in the case of 20 ns pulses; in fact, the SF growth length is expected to be larger for longer duration, lower intensity laser pulses [23]. Moreover, since SF is a non-linear, threshold process which enhances the intrinsic variability of the multimode laser pulse, it would account for the observed non-linear dependence of X-ray yield upon laser energy, for the X-ray pulse shortening with respect to the laser pulse, and for the shot-by-shot variability of the X-ray yield, which are all observed for both 3 ns and 20 ns laser pulses.

The correlation between SF, filamentation and X-ray production is presently being investigated by means of comparison between source images and spectra in the X-ray, optical and infrared regions of the spectrum of the plasma emission. Preliminary measurements [24] of the intensity of laser light scattered from the plasma, performed in a lower laser energy regime, have shown that the maximum of the X-ray yield with respect to the target position corresponds to a minimum in scattered light, suggesting that SF is active in maximising absorption of laser light in the plasma.

Since SF leads to a maximum in the X-ray yield, it could be beneficial for optimisation of X-ray conversion efficiency for laser plasma X-ray sources; however, it should be pointed that SF also introduces a large shot-by-shot variability of the X-ray yield. Actually, aluminium is not recommended as a target material for an efficient LPP X-ray source, since the X-ray conversion efficiency is relatively low. However, the use of aluminium allowed us to use K-shell spectroscopy as a plasma diagnostic, leading to a straightforward measure of the plasma temperature. Moreover, copper was also studied as a target material [18]; the observed features of the X-ray emission were similar to the ones we have discussed in this paper for aluminium targets, suggesting that SF was also probably effective; on the other hand, a considerably higher X-ray conversion efficiency was found. It is also interesting to notice that thermal SF is expected to be stronger in higher-Z materials, since the growth length scales as Z^{-1} [23]. Thus we believe that the information outlined in this paper for the optimisation of X-ray sources could be extended to target materials which are more interesting for application purposes.

5. – Conclusions

We analysed time-resolved spectra of *K*-shell line emission from aluminium laser-produced plasmas. Spectral characteristics of the X-ray emission were studied for laser pulses of two different duration and for different positions of the target along the laser beam propagation axis. The maximum X-ray yield position was found with the target displaced from the nominal focused beam waist, the displacement being larger for longer duration, lower intensity laser pulses. In this position an increase of plasma temperature was also observed. These features suggest that X-ray conversion efficiency is influenced by self-focusing of laser light in the plasma. This conclusion is supported by analogies with previous studies on laser light filamentation in the expanding plasma.

* * *

We acknowledge the support of R. Ripoli and the IFAM technical staff. We also thank C. Beneduce and R. Mildren for giving the preliminary results on the laser light scattering from the plasma and for useful suggestions about the manuscript. This work was fully supported by the Consiglio Nazionale delle Ricerche.

REFERENCES

[1] KAUFFMAN R., in *Handbook of Plasma Physics 3*, edited by M. N. ROSENBLUTH and R. SAGDEEV (North-Holland, Amsterdam) 1992.
[2] HAUER A. and BALDIS H. A., *Proceedings of the XLI SUSSP, St. Andrews, Scotland, 1994* (SUSSP Publications, Edinburgh) 1995.
[3] KEY M. H., LEWIS C. L. S., LUNNEY J. G., MOORE A., WARD J. M. and THAREJA R. K., *Phys. Rev. Lett.*, **44** (1980) 1669.
[4] YOUNG B. K. F., STEWART R. E., CERJAN C. J., CHARATIS G. and BUSCH G. E., *Phys. Rev. Lett.*, **61** (1988) 851.
[5] GIZZI L. A., GIULIETTI D., GIULIETTI A., AFSHAR-RAD T., BIANCALANA V., CHESSA P., DANSON C., SCHIFANO E., VIANA S. M. and WILLI O., *Phys. Rev. E*, **49** (1994) 5628; **50** (1994) 4266.
[6] HAUER A., MEAD W. C., WILLI O., KILKENNY J. D., BRADLEY D. K., TABATABATEI S. D. and HOOKER C. J., *Phys. Rev. Lett.*, **31** (1984) 2563.
[7] GIZZI L. A., MCKINNON A. J., RILEY D., VIANA S. M. and WILLI O., *Laser Part. Beams*, **13** (1995) 511.
[8] EDWARDS J., BARROW V., WILLI O. and ROSE S. J., *Europhys. Lett.*, **11** (1990) 631.
[9] NICOLOSI P., JANNITTI E. and TONDELLO G., *Appl. Phys. B*, **26** (1981) 117.
[10] TALLENTS G. J., LUTHER-DAVIES B. and HORSBURGH M. A., *Austr. J. Phys*, **39** (1986) 253.
[11] TURCU I. C. E., DAVIS G., GOWER M., O'NEILL F. and LAWLESS M., *Microelectron. Eng.*, **6** (1987) 287.
[12] O'NEILL F., in *Laser-Plasma Interaction 4, Proceedings of the XXXV SUSSP*, edited by M. B. HOOPER (SUSSP Publications, Edinburgh) 1988.
[13] HERRLIN K., SVAHN G., OLSSON C., PETTERSSON H., TILLMAN C., PERSSON A., WAHLSTROM C. G. and SVANBERG S., *Radiology*, **189** (1993) 65.
[14] TURCU I. C. E., TALLENTS G. J., ROSS I. N., MICHETTE A. G., SCHULTZ M. S., MELDRUM R. A., WHARTON C. W., BATANI D., MARTINETTI M. and MAURI A., *Phys. Medica*, **10** (1994) 93.

[15] LEE R. W., WHITTEN B. L. and STOUT R. E., *J. Quantum Spectrosc. Radiat. Transfer*, **32** (1984) 91.
[16] BATANI D., BIANCALANA V., CHESSA P., DEHA I., GIULIETTI A., GIULIETTI D. and GIZZI L. A., *Nuovo Cimento D*, **15** (1993) 753.
[17] DUSTON D., CLARK R. W., DAVIS J. and APRUZESE J. P., *Phys. Rev. A*, **27** (1983) 1441.
[18] BASTIANI S., GIULIETTI D., GIULIETTI A., GIZZI L. A., CECCOTTI T. and MACCHI A., *Laser Part. Beams*, **13** (1995) 493.
[19] GIULIETTI D., BASTIANI S., CECCOTTI T., GIULIETTI A., GIZZI L. A and MACCHI A., *Nuovo Cimento D*, **17** (1995) 401.
[20] GRIEM H. R., in *Handbook of Plasma Physics*, edited by M. N. ROSENBLUTH and R. SAGDEEV, Vol. **1** (North-Holland, Amsterdam) 1983.
[21] BIANCALANA V., BORGHESI M., CHESSA P., DEHA I., GIULIETTI A., GIULIETTI D., GIZZI L. A and WILLI O., *Europhys. Lett.*, **22** (1993) 175.
[22] EPPERLEIN E. M., *Phys. Rev. Lett.*, **65** (1990) 2145.
[23] GIULIETTI D., LUCCHESI M., GIULIETTI A. and VASELLI M., *J. Appl. Phys.*, **58** (1985) 2961.
[24] MACCHI A., BASTIANI S., BENEDUCE C., GIULIETTI A., GIULIETTI D., GIZZI L. A. and MILDREN R., contribution to *II Euroconference on Generation and Application of Ultrashort X-ray Pulses, Pisa, September 1995* (unpublished).